High Water–Gas Shift Activity in TiO2(110) Supported Cu and Au Nanoparticles: Role of the Oxide and Metal Particle Size

ARTICLE *in* THE JOURNAL OF PHYSICAL CHEMISTRY C · APRIL 2009

Impact Factor: 4.77 · DOI: 10.1021/jp900483u

THE JOURNAL OF PHYSICAL CHEMISTRY C

Article

High Water#Gas Shift Activity in TiO(110) Supported Cu and Au Nanoparticles: Role of the Oxide and Metal Particle Size

Jose# A. Rodri#guez, Jaime Evans, Jesu#s Graciani,
Joon-Bum Park, Ping Liu, Jan Hrbek, and Javier Fdez. Sanz

J. Phys. Chem. C, **2009**, 113 (17), 7364-7370• DOI: 10.1021/jp900483u • Publication Date (Web): 08 April 2009

High Water−Gas Shift Activity in TiO_2(110) Supported Cu and Au Nanoparticles: Role of the Oxide and Metal Particle Size

José A. Rodríguez,*,† Jaime Evans,‡ Jesús Graciani,†,§ Joon-Bum Park,† Ping Liu,† Jan Hrbek,† and Javier Fdez. Sanz*,§

Chemistry Department, Brookhaven National Laboratory, Upton, New York 11973, USA, Facultad de Ciencias, Universidad Central de Venezuela, Caracas 1020 A, Venezuela, and Departamento de Química Física, Facultad de Química, Universidad de Sevilla, E-41012, Sevilla, Spain

Received: January 16, 2009; Revised Manuscript Received: February 20, 2009

The deposition of Cu and Au nanoparticles on TiO_2(110) produces very good catalysts for the WGS. Although bulk metallic gold is not active as a WGS catalyst, Au nanoparticles supported on TiO_2(110) have an activity comparable to that of Cu/ZnO(000$\bar{1}$). Cu/TiO_2(110) is clearly a better catalyst than Cu/ZnO(000$\bar{1}$) or Au/TiO_2(110). The catalysts that have the highest activity for the WGS have also the lowest apparent activation energy. On Cu(111) and Cu(100), the aparent activation energies are 18.1 and 15.2 kcal/mol, respectively. The apparent activation energy decreases to 12.4 kcal/mol on Cu/ZnO(000$\bar{1}$), 10.2 on Au/TiO_2(110), and 8.3 kcal/mol on Cu/TiO_2(110). The Cu ↔ titania interactions are substantially stronger than the Au ↔ titania interactions. This has an effect on the growth mode of the metals on TiO_2(110). In images of scanning tunneling miscroscopy, the average particle size in Cu/TiO_2(110) is smaller than that in Au/TiO_2(110). The Cu particles are dispersed on the terraces and steps of the oxide surface, whereas the Au particles concentrate on the steps. The morphology of Cu/TiO_2(110) favors high catalytic activity. The results of density functional calculations indicate that the metal−oxide interface plays an essential role in the catalysis, helping in the dissociation of water and in the formation of an OCOH intermediate, which decomposes to yield CO_2 and hydrogen.

I. Introduction

Hydrogen is a potential solution for satisfying many of our energy needs.[1] At present, nearly 95% of the hydrogen supply is produced from the reforming of crude oil, coal, natural gas, and biomass.[2] The reformed fuel contains 1−10% of CO, which degrades the performance of the Pt electrodes utilized in the fuel cell systems. This is the reason why the water−gas shift reaction (WGS, $CO + H_2O \leftrightarrow CO_2 + H_2$) plays a key role for getting clean hydrogen for both fuel cells and other industrial applications.

Currently, Cu based catalysts, both pure and supported on metal-oxides, fall among the more active and promising for the water−gas shift reaction although their performance is not fully understood and is highly dependent on the synthesis conditions or the nature of the oxide support.[3,4] Either metallic Cu or Cu^+ cations have been proposed as the active sites for the WGS reaction.[3] Oxide mixtures of CuO−ZnO or CuO−ZnO/Al_2O_3 are the commercially used WGS catalysts at temperatures between 450−525 K. However, these oxide catalysts are pyrophoric and normally require lengthy and complex activation steps before usage.[3] It is desirable to find oxide supports that have a performance superior to that of ZnO. Titania is a nonexpensive and environmetally benign oxide with well-known physical and chemical properties.

In a recent article, we have shown the existence of a Au ↔ N synergism on N-doped titania.[5] This phenomenon, while stabilizing N atoms implanted in the TiO_2 lattice, formally leads to cationic $Au^{\delta+}$ species on the surface as a consequence of an electron transfer between the transition metal and N levels.[5] The Au/N−TiO_2(110) system was found to be more active for the WGS reaction than for undoped Au−TiO_2 materials,[6,7] and even better than Cu, the most active transition-metal catalyst. These findings suggested to us that TiO_2-supported Cu particles could also be active in WGS because the more electropositive character of Cu makes it more prone to get oxidized on the surface.[8] In this work, we study the production of hydrogen through the WGS reaction on model catalysts consisting of Cu particles supported on TiO_2 and ZnO surfaces and compare their activity with similar Au-based phases. We find that the deposition of copper on TiO_2(110) leads, as in the case of Au/N−TiO_2(110),[5] to metal cationic centers on the surface and that it results in a much better WGS catalyst than Cu/ZnO(000$\bar{1}$). We observe that the WGS activity is affected by the metal particle size, the metal ↔ TiO_2 interactions, and the reducibility of the titania surface.

II. Experimental and Theoretical Methods

A. Scanning Tunneling Microscopy, Photoemission, and Tests of Catalytic Activity. The microscopy studies were carried out in an Omicron variable temperature STM system that is directly attached to a main ultrahigh vacuum (UHV) chamber equipped with optics for low-energy electron diffraction, instrumentation for Auger electron spectroscopy, surface cleaning facilities, and an e-beam metal evaporator for Cu. Chemically etched W tips were used for imaging the surfaces. The TiO_2(110) crystal, from Princeton Scientific Corporation, was cleaned by several cycles of Ne^+ sputtering (1 keV, 40 min) and annealing (950 K, 5 min), and XPS/AES studies confirmed that there were no surface contaminants after this treatment.[9] Furthermore, the high-resolution STM images of the

† Brookhaven National Laboratory.
‡ Universidad Central de Venezuela.
§ Universidad de Sevilla.

10.1021/jp900483u CCC: $40.75
Published on Web 04/08/2009

surface exhibited bright Ti rows separated by 6.5 Å, as typically observed for TiO_2(110)-(1 × 1).[10] Cu was vapor-deposited on the surface from a homemade doser consisting of a Cu wire (Alfa Aesar, 99.999%), which was heated by passing current through tungsten wire wrapped by the Cu wire.

Photoemission studies were performed at beamline U7A of the National Synchrotron Light Source (NSLS) at Brookhaven National Laboratory[7] using a photon-energy of 625 eV to collect the O 1s and Ti 2p regions, and 325 eV to collect the C 1s, Au 4f, and valence regions. In a separate UHV chamber, we acquired XPS spectra (Cu 2p, Ti 2p, O 1s, C 1s, and Au 4f regions) and UPS spectra (valence region) using Mg Kα and He−I radiation, respectively.[7]

The tests of catalytic activity were performed in an ultrahigh-vacuum (UHV) chamber that has attached a high-pressure cell or batch reactor.[7,11] Au and Cu were vapor deposited on a TiO_2(110) following the methodology described in refs 12 and 13. The deposition of the admetals was performed at room temperature, with subsequent heating of the Au/TiO_2(110) and Cu/TiO_2(110) surfaces to the temperatures used for studying the WGS reaction (575−650 K). The WGS activity of the samples was investigated with a mixture of 20 Torr of CO and 10 Torr of H_2O.[7,11] The CO gas was cleaned of any metal carbonyl impurity by passing it through purification traps.

B. Density Functional Calculations. Density functional (DF) calculations have been performed to investigate the interaction of Au_8 and Cu_8 clusters with a TiO_2(110) substrate using the plane-wave-pseudopotential approach within the projector augmented wave method,[14] together with the PW91-GGA exchange correlation functional as implemented in the *VASP 4.6* code.[15] The cutoff for the plane waves was 400 eV. The Ti (3d, 4s), O (2s, 2p), N (2s, 2p), Au (5d, 6s), and Cu (3d, 4s) electrons were explicitly treated as valence states. The calculations were carried out at the Γ point using the Gaussian smearing method, with an electronic temperature of $k_BT = 0.1$ eV. All energies were extrapolated to $T = 0$ K. The TiO_2(110) surface was represented by slabs generated from a supercell made of 4 × 2 unit cells, six layers thick ($Ti_{96}O_{192}$). For more details see ref 5 and 16.

We also investigated the energetics for the WGS reaction on Au/TiO_2(110) and Cu/TiO_2(110) surfaces. In this case, we used 4 × 2 unit cells with a slab thickness reduced to three layers. To be able to directly compare with results reported in the literature,[7,17] the unresticted DF calculations for the WGS were carried out with the *DMol*^{3} code[18] treating molecules, nanostructures, and extended surfaces with the same level of accuracy. The ionic cores were described by effective core potentials (ECP). A numerical basis set was used with comparable accuracy to a Gaussian 6-31G (d) basis set.[18] A local basis cutoff of 5.0 Å in real space was employed. This basis set and cutoff were used in previous studies dealing with Au nanoparticles and gave a very good description of their properties.[7,17] The PW91-GGA exchange correlation functional was also utilized in the *DMol*^{3} calculations. The top O−Ti−O layer of the oxide surface and the metal nanoparticles were allowed to fully relax with the adsorbates. Enough K-points (9) were selected for the surfaces. Transition states here were identified using the combination of synchronous transit methods and eigenvector following and verified by the presence of a single imaginary frequency from a sequential vibrational frequency analysis.[19] Our objective here is to obtain a semiquantitative description of the energetics for the WGS on Au/TiO_2(110) and Cu/TiO_2(110) surfaces.[7,17] In the past, we have found that DF calculations with *VASP* and *DMol*^{3} give very similar trends for the energetics of surface reactions.[20,21]

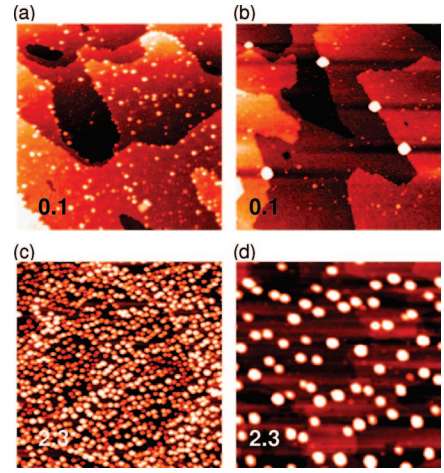

Figure 1. Set of 150 × 150 nm^2 STM images of Cu deposited on TiO_2 (110) with different Cu coverages and sample temperatures (a) 0.1 ML of Cu at 298 K, (b) 0.1 ML of Cu after annealing at 625 K for 10min, (c) 2.3 ML of Cu at 298 K, and (d) 2.3 ML of Cu after annealing at 625 K for 10min. Cu was deposited at 298 K and all STM images were obtained at 298 K (2.5 V, 0.05 nA).

III. Results

A. Growth Mode of Cu and Au Nanoparticles on TiO_2(110). Studies have been published examining in detail the deposition of small amounts of Au on TiO_2(110) with scanning tunneling microscopy.[22,23] These studies indicate that Au grows on this oxide substrate forming 3D particles. At 300 K, the Au clusters nucleate mainly on step sites or on defect sites present in the terraces of TiO_2(110). The interaction of Au with an ideally flat TiO_2(110) surface is quite weak,[5,12,24] and a substantial amount of particle sintering occurs when the system is annealed from 300 to 650 K.[22,23]

Figure 1 shows STM images obtained after depositing 0.1 and 2.3 ML of Cu on TiO_2(110). The deposition of Cu at room temperature, panels (a) and (c), produces surfaces in which the Cu particles are well dispersed on the terraces. This is quite different from the nucleation at step sites observed for Au/TiO_2(110).[22,23] Even after annealing to 625 K, panels (b) and (d), one finds a large fraction of Cu particles on the titania terraces. Using the STM images, one can estimate the diameter and height of the clusters, dimensions which are correlated.[9,23,25] In general, the height can be evaluated in a more precise way with STM.[9,23,25] For the surface with 0.1 ML of Cu annealed to 625 K, one finds a bimodal distribution of cluster sizes: small clusters with a height bellow 1 nm (top panel in Figure 2) and big clusters with a height around 2.3 nm (not shown in Figure 2). In the case of a surface with 2.3 ML of Cu annealed to 625 K, big clusters are seen with a height around 3.2 nm (bottom panel of Figure 2). This result is consistent with previous STM images for large coverages of Cu on TiO_2(110).[26] As we will see below, the size and dispersion of the Cu nanoparticles have a significant effect on their activity for catalyzing the water−gas shift reaction.

In the past, our group has examined the interaction of a Au atom and a Au_8 cluster with a perfect TiO_2(110) surface using DF calculations.[5] The adsorption energies for Au and Au_8 were −0.18 and −0.24 eV, respectively. At the bottom of Figure 3 is shown the most stable structure for Au_8/TiO_2(110). The Au cluster is weakly bound and essentially can move freely on the

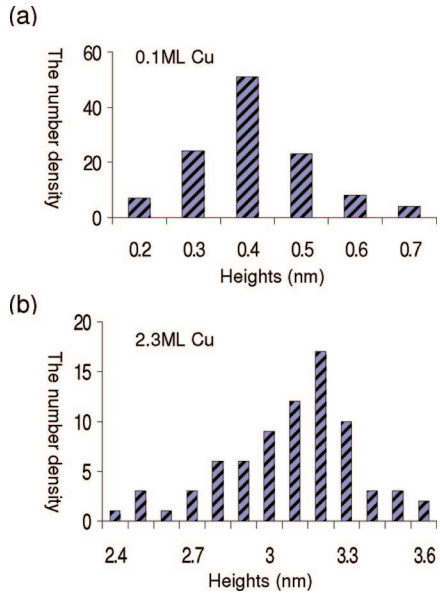

Figure 2. Histograms for the distribution of heights of the Cu nanoparticles shown in parts b and d of Figure 1. (a) Cu/TiO_2(110) surface with 0.1 ML of Cu after annealing at 625 K. Note that the big Cu nanoclusters with an average height of 2.3 nm are not included in the graph. (b) Cu/TiO_2(110) surface with 2.3 ML of Cu after annealing at 625 K.

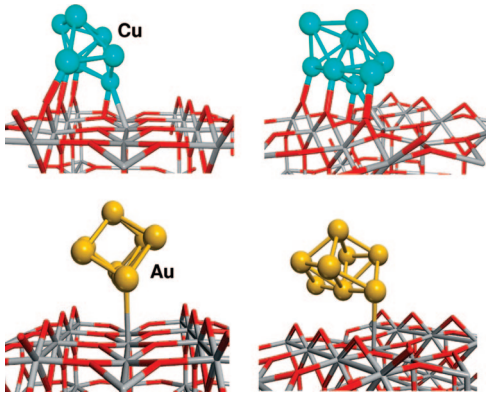

Figure 3. Calculated structures for the interaction of Cu_8 (top, blue spheres) and Au_8 (bottom, yellow spheres) with TiO_2(110). The structure for Au_8/TiO_2(110) was taken from ref 5. We are showing two different perspectives for each system. The red sticks represent O, while gray sticks denote Ti. Only the top layers of the six-layer titania slab used in the DF calculations are shown.

oxide surface. This is consistent with other theoretical studies[24,27] and it explains why the deposited Au grows on steps and defects of TiO_2(110).[22,23] The presence of O vacancies on TiO_2(110) drastically increases the adsorption energy of Au.[5,24,27] With these results as a background, we proceeded to study the bonding of a Cu atom and a Cu_8 cluster to TiO_2(110). The Cu atom was preferentially adsorbed on two bridging O atoms of the titania substrate with a bonding energy of −1.76 eV. The Cu_8 cluster was bound to the TiO_2(110) surface in a similar way. It interacted mainly with the protruded oxygen atoms, see top of Figure 3, and adopted a quasi-two-layer structure. The adsorption energy of Cu_8 was −3.34 eV.

A Bader analysis of the electron density[28] showed that Cu atoms belonging to the contact layer were charged (∼0.5 |e|), whereas those of the upper layer were almost neutral. On the basis of the DF results, it is not surprising that Cu particles bind well to the terrace sites of TiO_2(110) as seen in the STM figures of Figure 1. The Cu ↔ TiO_2(110) interactions are much

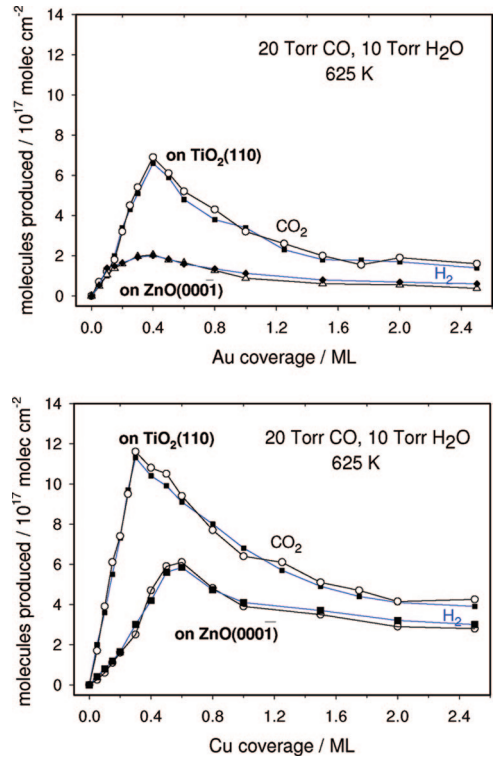

Figure 4. WGS activity of model Au/TiO_2(110) and Cu/TiO_2(110) catalysts as a function of admetal coverage. Each surface was exposed to a mixture of 20 Torr of CO and 10 Torr of H_2O at 625 K for 5 min. Steady state was reached 2−3 min after introducing the gases in the batch reactor.

stronger than the Au ↔ TiO_2(110) interactions. Furthermore, Au prefers to bind to O vacancies of TiO_{2-x}(110)[24,27] but this is not the case for Cu on TiO_{2-x}(110). The calculated bonding energy for a Cu atom on a fully stoichiometric TiO_2(110) surface is −1.76 eV, and only −0.94 eV on an O vacancy of TiO_{2-x}(110) (decrease of 47% in the adsorption energy). Thus, in the copper/titania and gold/titania systems one has quite different metal ↔ oxide interactions, which affect the size, dispersion, and surface position of the metal particles.

B. Water−Gas Shift Reaction on Cu/TiO_2(110) and Au/TiO_2(110) Surfaces: Kinetic Studies. Whereas pure copper surfaces are active catalysts for the water−gas shift (WGS),[29] neither Au(111) nor TiO_2(110) are able to catalyze this reaction. The catalytic activity of (Au,Cu)/TiO_2(110) versus the metal loading of Au or Cu is reported in Figure 4. As can be seen, the activity appears and increases as Au and Cu are added, reaching a maximum at admetal coverages of 0.3−0.4 ML. For metal coverages above 0.5 ML, the catalytic activity decreases when the coverage of Au or Cu increases. After normalizing the amount of H_2/CO_2 molecules produced by the total number of Cu atoms present in the surface, one finds that the small particles in part a of Figure 2 (<1 nm in height) are much more reactive than the big particles in part b of Figure 2 (>2.5 nm in height). Size also affects the reactivity of the Au particles on TiO_2(110).[22,23] A substantial fraction of the admetal particles have a height below 1 nm at a coverage of 0.2 ML when the surfaces exhibit very high catalytic activity on a per metal atom basis. The drop in catalytic activity at coverage above 0.6 ML is probably associated with an increase in particle size.[22,23] As the particle size increases, the metal particles may be exposing more stable faces of the bulk metals in which the atoms have a large number of neighbors, and the WGS is a structure

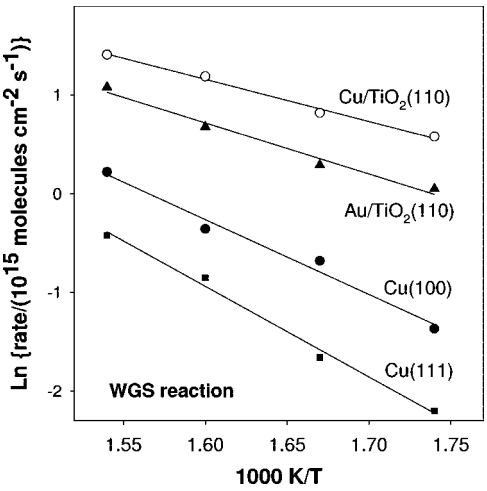

Figure 5. Arrhenius plot of the WGS reaction rate for Cu(111), Cu(100), 0.4 ML of Au on TiO_2(110), and 0.5 ML of Cu on TiO_2(110). The data were acquired with a pressure of 20 Torr of CO and 10 Torr of H_2O.

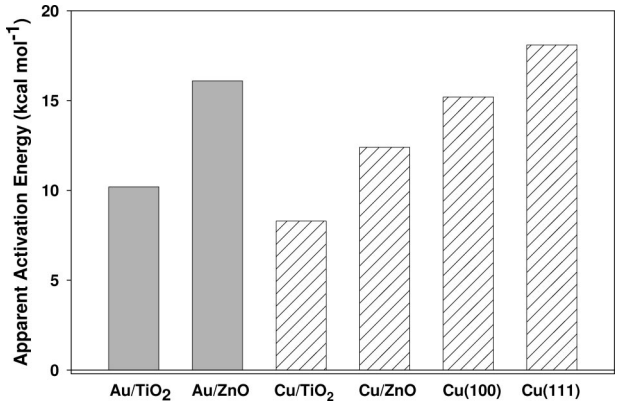

Figure 6. Apparent activation energies observed for the WGS over Au/TiO_2(110), Au/ZnO(000$\bar{1}$),[7] Cu/TiO_2(110), Cu/ZnO(000$\bar{1}$),[7] Cu(100), and Cu(111).

sensitive reaction that proceeds faster on surfaces which exhibit metal centers with a relatively low coordiantion.[17,29]

The Cu/ZnO system is frequently used as a WGS catalyst in industrial operations.[3,6] In Figure 4, we also include data previously reported for the WGS activity of Au/ZnO(000$\bar{1}$) and Cu/ZnO(000$\bar{1}$).[7] The order of activity for the metal/oxide catalysts follows the trend: Au/ZnO < Cu/ZnO $\approx$ Au/TiO_2 < Cu/TiO_2.

Cu/TiO_2 is clearly a much better WGS catalyst than Cu/ZnO, being $\sim$2 times more active when comparing maximum activities. Postreaction surface analysis with XPS showed that the copper and gold in the metal/oxide catalysts remained in a metallic state. This is consistent with previous in situ measurements of X-ray absorption spectroscopy for high-surface area WGS catalysts that contain copper and gold.[6,11,30−32] Ti 2p core-level XPS spectra showed partial reduction of the titania support, TiO_{2-x} $x = 0.09-0.13$, after exposing Cu/TiO_2(110) and Au/TiO_2(110) to the WGS reaction mixture or CO. This reduction was not observed when pure TiO_2(110) was exposed to the gases. Thus, it appears that the admetals promote the formation of O vacancies in titania. As we will see below, the O vacancies could participate directly in the activation of the Au nanoparticles[24,27] or in the dissociation of water. Interestingly, surface characterization of Cu/ZnO(000$\bar{1}$) and Au/ZnO(000$\bar{1}$) after the WGS reaction did not find a measurable number of O vacancies in the oxide support.[7] Such an absence of O vacancies could explain the substantial difference between the catalytic activity of the systems containing zinc oxide and systems containing titania. The reducibility of the oxide support is an important factor to consider when explaining the activity of noble-metal catalysts (Pt, Rh, Ru, and Pd) dispersed on polycristalline titania powders.[33,34]

Experiments similar to those in Figure 4 were also done at temperatures of 575, 600, and 650 K for the WGS on Cu/TiO_2(110) and Au/TiO_2(110) at an admetal coverage of 0.4 ML. Using the ln of the reaction rates, we constructed Arrhenius plots for the two catalysts. Figure 5 summarizes the results together with data for Cu(100) and Cu(111).[7] Although Cu(111) is not very active as a catalyst for the WGS, it is frequently used as a benchmark.[6,35] Note that Au(111) or polycrystalline Au do not have any catalytic activity.[7] In Figure 5, Cu/TiO_2(110) is the best WGS catalyst at all temperatures. The Cu nanoparticles supported on titania generate a catalyst which is 6 (at 650 K) to 16 times (at 575 K) more active than Cu(111). In general, Au/TiO_2(110) is not as good a catalyst as Cu/TiO_2(110), but its performance is still quite remarkable because neither Au(111) nor polycrystalline Au are able to catalyze the WGS. On the basis of the dispersion observed for the metal in Cu/TiO_2(110), see Figure 1, and Au/TiO_2(110), see refs 23 and 22, one would expect the former to be more catalytically active because the Cu particles are dispersed on the terraces and steps, whereas the Au particles are localized only at steps and other surface defects. According to the DF calculations, Au particles will block O vacancies in TiO_{2-x}(110), whereas the Cu particles will let the O vacancies free for interaction with adsorbates. The higher the gold coverage on the surface, the lower the number of exposed O vacancies in titania.[24,25]

Figure 6 displays the apparent activation energies for a series of Au and Cu catalysts. On Cu(111) and Cu(100), the apparent activation energies are 18.1 and 15.2 kcal/mol, respectively. The apparent activation energy decreases to 12.4 kcal/mol on Cu/ZnO(000$\bar{1}$)[7] and 8.3 kcal/mol on Cu/TiO_2(110). For the Au systems, the aparent activation energies are 16.1 kcal/mol on Au/ZnO(000$\bar{1}$)[7] and 10.2 kcal/mol on Au/TiO_2(110). The catalysts that have the highest activity in Figure 4 have the lowest apparent activation energy in Figure 6. These data corroborate the benefits of using titania as a support.

To date, two main reaction mechanisms have been proposed for the WGS on metal/oxide surfaces.[3,6] One is a redox mechanism, where CO reacts with an oxygen atom coming from water dissociation or the oxide support to form CO_2. The other is an associative mechanism where the main reaction intermediates are species such as formate, carbonate, or carboxyl, produced by reaction of CO with terminal hydroxyl groups present in the surface of the catalyst. In the case of Cu(100) and Cu(111),[7,29] analysis of the surfaces after the WGS reaction showed them to be essentially free of formate and carbonate species. On these extended copper surfaces, the reaction probably proceeds through a redox mechanism.[7,29] This may not be the case for Cu/TiO_2(110) and Au/TiO_2(110). XPS characterization of these metal/oxide surfaces after the WGS reaction gave the typical peaks for adsorbed formate- or carbonate-like species in the C 1s region. Therefore, the XPS data opens the possibility for an associative mechanism, although the formate- or carbonate-like species could be simply spectators bound to the oxide. In the next section, we will use DF calculations to study the WGS reaction on Au/TiO_{2-x}(110) and Cu/TiO_{2-x}(110) surfaces.

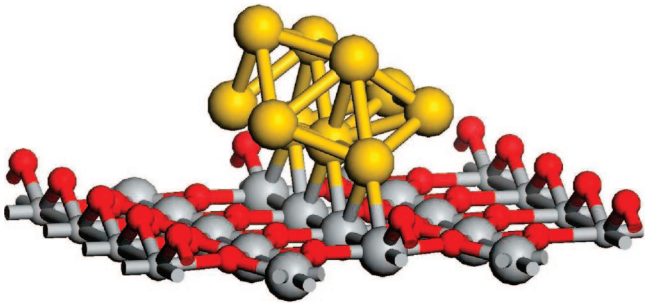

Figure 7. Relaxed geometry for a Au_{10} cluster supported on partially reduced TiO_2(110). The gold atoms are shown as yellow spheres. Red spheres represent O atoms, whereas gray spheres denote Ti atoms. Only the top layer of the three-layer titania slab used in the DF calculations is partly shown.

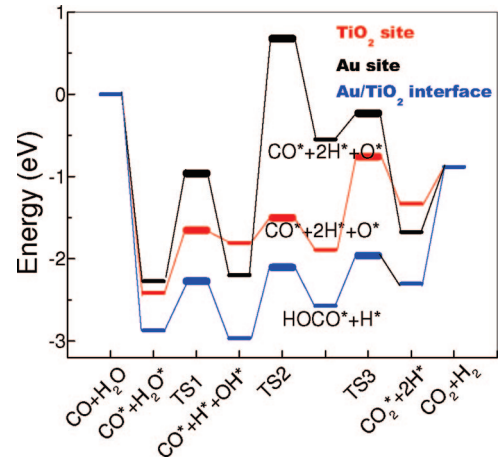

Figure 8. Calculated reaction profile for the WGS on the model catalyst shown in Figure 7. The zero energy is taken as the sum of the energies of the bare gold−titania system, gas-phase water, and carbon monoxide. The reaction path was examined on top of the Au nanoparticle (Au site, black lines), on the titania support (TiO_2 site, red lines), and at the Au/TiO_2 interface (blue lines). The corresponding structures for the calculations at the Au/TiO_2 interface are shown in Figure 9. Transition states are labeled TS.

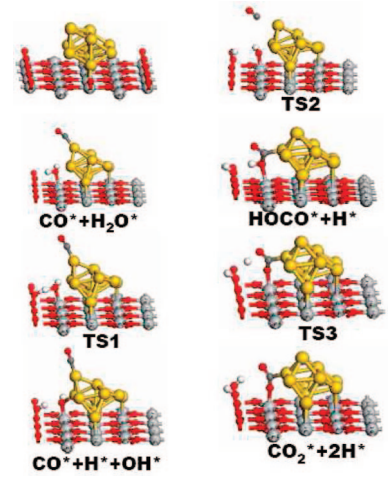

Figure 9. Calculated structures for the reactants and intermediates of the WGS reaction on the model catalyst of Figure 7. Color code: Yellow, gold; white, hydrogen; dark gray, carbon; red, oxygen; soft gray, titanium. Transition states are labeled TS. Only the top layer of the three-layer titania slab used in the DF calculations is shown.

C. Reaction Mechanism for the Water−Gas Shift on Cu/TiO_{2-x}(110) and Au/TiO_{2-x}(110): Density Functional Studies. One remarkable result in Figures 4 and 5 is the high catalytic activity of Au/TiO_{2-x}(110). A previous DF study has examined the energetics for the WGS reaction on a Au(100) surface and on gold nanoparticles.[17] None of these systems is able to catalyze the reaction due to a very large barrier for the dissociation of H_2O. When this result is compared to the kinetic data in Figures 4 and 5, it suggests a direct participation of the titania support in the WGS process. The XPS data show that titania is partially reduced after performing the WGS on Au/TiO_2(110). The O vacancies of TiO_{2-x}(110) can play a direct role in the dissociation of H_2O[36,37] but the presence of Au binding at O vacancy sites blocks the dissociative chemisorption of the molecule.[38] To represent the Au/ TiO_{2-x}(110) surface, we used the model proposed by Nørskov et al.[24,27] In this model, a Au_{10} cluster is anchored on three O vacancies of a reduced titania surface, as seen in Figure 7. The Au_{10} cluster has a diameter of ∼0.7 nm, and it should be at the lower end of the size range for active Au nanoparticles.[22,23] The model in Figure 7 contains the characteristic (111) and (100) facets of gold clusters and it takes into account the finite size of the cluster and the redox character of the titania support.[24]

Figure 8 shows the calculated energy changes for the WGS reaction on a Au/TiO_{2-x}(110) surface. We have considered reaction on sites of the supported Au_{10} particle, on sites of the titania support not covered by gold, and on the gold−titania interface. The reaction pathway with the minimum energy barriers is seen at the gold−titania interface and involves the following steps:

$$CO_{gas} \leftrightarrow CO_{ads} \quad (1)$$

$$H_2O_{gas} \leftrightarrow H_2O_{ads} \quad (2)$$

$$H_2O_{ads} \leftrightarrow OH_{ads} + H_{ads} \quad (3)$$

$$CO_{ads} + OH_{ads} \rightarrow OCOH_{ads} \quad (4)$$

$$OCOH_{ads} \rightarrow CO_{2,gas} + H_{ads} \quad (5)$$

$$2H_{ads} \rightarrow H_{2,gas} \quad (6)$$

The corresponding structures for the different adsorbates are displayed in Figure 9. The chemisorption of water and CO is a very exothermic process and the released energy can be used to overcome the energy barriers for the dissociation of water, eq 3, the formation of the OCOH intermediate, eq 4, and its dissociation into CO_2 and atomic H, eq 5. The activation barrier for the dissociation of H_2O at the gold−titania interface is substantially smaller than on the supported gold nanoparticle (1.3 eV vs 0.6 eV). On the titania sites, we calculate an activation barrier of 0.6 eV for the dissociation of water, which can go down to only 0.3 eV when the surface is not covered with CO.[37] The formation of a OCOH intermediate is only seen at the gold−titania interface. On the other two types of reaction sites, the WGS follows a redox mechanism with full dissociation of water before a CO ↔ O interaction. Reaction paths involving the formation of formate, HCOO, or carbonate had the energy barriers higher than 2 eV and could not compete with the reaction paths shown in Figure 8. Thus, the formate or carbonate species detected with XPS after performing the WGS reaction on Au/TiO_{2-x}(110) are probably spectators.

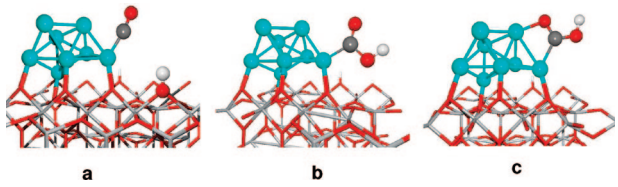

Figure 10. Calculated structures for the reaction of CO and OH on the model Cu/TiO_2(110) catalyst of Figure 3. Initially (a), CO is bound to the Cu_8 cluster, whereas OH is above an O vacancy of the titania surface. Color code: Blue, copper; white, hydrogen; dark gray, carbon; red, oxygen; soft gray, titanium.

In Figure 9, gold and oxide sites cooperate in the partial dissociation of water, and the formation and dissociation of the OCOH intermediate. These cooperative interactions are essential for the high catalytic activity of the Au/TiO_{2-x}(110) surface as seen in Figure 8. Previous theoretical studies have shown that cooperative interactions at the gold−titania interface are quite important for the oxidation of CO ($2CO + O_2 \leftrightarrow 2CO_2$)[22] and DeSOx reactions ($SO_2 + 2CO \leftrightarrow S + 2CO_2$).[12] In the case of the WGS, no catalytic activity is seen if the oxide is not present.[7,17]

Cu(100) and Cu(111) interact with the water molecule much better than Au(111),[17,35] and, therefore, these copper surfaces are able to catalyze the WGS reaction. Still, DF calculations point to the dissociation of water as the rate-determining step for the WGS on Cu(100) and Cu(111).[17,35] In Figure 6, the reduction in the apparent activation energy when going from Cu(100) or Cu(111) to Cu/TiO_{2-x}(110) is probably a consequence of a decrease in the barrier for the dissociation of water. There is a low activation barrier for the dissociation of water on O vacancies of titania (~0.35 eV)[37] and copper does not cover these sites preferentially as gold does (above). An activation barrier of 0.35 eV is significantly smaller than the activation barrier of 1.1−1.3 eV calculated for the dissociation of water on Cu surfaces.[17,35] In the present context, such a low value indicates that the water O−H bond cleavage is no longer the rate limiting step and we must look further to get a consistent description of the catalytic process. According to the theoretical mechanistic studies performed so far,[17,35] the next more costly step is the reaction between coadsorbed OH and CO species to give an adsorbed OCOH species, as seen in eq 4. To address this issue, we performed DF calculations on a catalyst model consisting of a Cu_8 cluster supported on a TiO_{2-x}(110) surface. We set up a model in which there is an OH adsorbed near the Cu_8 cluster, on which a CO molecule has also been preadsorbed (part a of Figure 10). It is worth noting that this is not the most stable arrangement for CO and OH, although the energy differences are small. For instance, the OH groups prefer to lie on the free bridging oxygen rows; however, the model has to be flexible enough to favor in some way the encounter of reactants. From this starting configuration, we considered moving the OH group from the surface toward the carbon atom that finally leads to the adsorbed carboxyl compound. The reaction formally appears to occur through a two-step process. The first gives a OCOH group bound to the Cu_8 cluster only through the carbon atom (part b of Figure 10), and in the second there is a bending of the carboxyl group that now is also bonded to the Cu_8 cluster through an oxygen−Cu bond (part c of Figure 10). Transition-state calculations showed that the first step involves a barrier height of 0.9 eV, whereas the second step is almost barrierless. The overall eq 10a → 10c is endothermic by 0.7 eV consistent with the result observed for Au/TiO_{2-x}(110) in Figure 8. However, it should be noticed that the reaction involves the regeneration of a surface vacancy that always is an energy-consuming process. The adsorption of CO and H_2O on the surface could release the energy necessary for the process shown in Figure 10.

Conclusions

In summary, the deposition of Cu and Au nanoparticles on TiO_2(110) produces very good catalysts for the WGS. Although bulk metallic gold is not active as a WGS catalyst, Au nanoparticles supported on TiO_2(110) have an activity comparable to that of Cu/ZnO(000$\bar{1}$). Cu/TiO_2(110) is clearly a better catalysts than Cu/ZnO(000$\bar{1}$) or Au/TiO_2(110). The catalyst that has the highest activity for the WGS has also the lowest apparent activation energy. On Cu(111) and Cu(100), the apparent activation energies are 18.1 and 15.2 kcal/mol, respectively. The apparent activation energy decreases to 12.4 kcal/mol on Cu/ZnO(000$\bar{1}$), 10.2 on Au/TiO_2(110), and 8.3 kcal/mol on Cu/TiO_2(110). This trend corroborates the benefits of using titania as a support.

The Cu ↔ titania interactions are substantially stronger than the Au ↔ titania interactions. This has an effect on the growth mode of the metals on TiO_2(110). In Cu/TiO_2(110), the average particle size is smaller than on Au/TiO_2(110). The Cu particles are dispersed on the terraces and steps of the oxide surface, whereas the Au particles concentrate on the steps. The morphology of Cu/TiO_2(110) favors high catalytic activity.

The metal−oxide interface plays an essential role in the catalysis, helping in the dissociation of water and in the formation of an OCOH intermediate which decomposes to yield CO_2 and hydrogen. Titania is efficient for the dissociation of water but binds O, formates, and carbonates too strongly. On the other hand, the metals have difficulty dissociating water but can easily perform the subsequent steps of the WGS.

Acknowledgment. This work was funded by the Ministerio de Educación y Ciencia, MEC, from Spain (project MAT2008-04918), and the Junta de Andalucía (project FQM-132). We also thank the computational resources provided by the Barcelona Supercomputing Center - Centro Nacional de Supercomputación (Spain) and the computing facilities at the Center for Functional Nanomaterials of Brookhaven National Laboratory. The work done at Brookhaven National Laboratory was supported by the U.S. Department of Energy, Division of Chemical Sciences (DE-AC02-98CH10886). J.E. thanks INTEVEP for a travel grant that made possible a part of this project.

References and Notes

(1) Jacobson, M. Z.; Colella, W. G.; Golden, D. M. *Science* **2005**, *308*, 1901.
(2) Spivey, J. J. *Catal. Today* **2005**, *100*, 171.
(3) Thomas, J. M.; Thomas, W. J. *Principles and Practice of Heterogeneous Catalysis*; VCH: New York, 1997.
(4) Fu, Q.; Saltsburg, H.; Flytzani-Stephanopoulos, M. *Science* **2003**, *301*, 935.
(5) Graciani, J.; Nambu, A.; Evans, J.; Rodriguez, J. A.; Sanz, J. F. *J. Am. Chem. Soc.* **2008**, *130*, 12056.
(6) Burch, R. *Phys. Chem. Chem. Phys.* **2006**, *8*, 5483.
(7) Rodriguez, J. A.; Liu, P.; Hrbek, J.; Evans, J.; Perez, M. *Angew. Chem., Int. Ed.* **2007**, *46*, 1329.
(8) (a) Hernandez, N. C.; Graciani, J.; Marquez, A.; Sanz, J. F. *Surf. Sci.* **2005**, *575*, 189. (b) Sanz, J. F.; Hernandez, N. C. *Phys. Rev. Lett.* **2005**, *94*, 016104.
(9) Park, J. B.; Ratliff, J. S.; Ma, S.; Chen, D. A. *J. Phys. Chem. C* **2007**, *111*, 2165.
(10) Diebold, U. *Surf. Sci. Rep.* **2003**, *48*, 53.
(11) Wang, X.; Rodriguez, J. A.; Hanson, J. C.; Pérez, M.; Evans, J. *J. Chem. Phys.* **2005**, *123*, 221101.

(12) Rodriguez, J. A.; Liu, G.; Jirsak, T.; Hrbek, J.; Chang, Z.; Dvorak, J.; Maiti, A. *J. Am. Chem. Soc.* **2002**, *124*, 5242.

(13) Zhao, X.; Hrbek, J.; Rodriguez, J. A.; Pérez, M. *Surf. Sci.* **2006**, *600*, 229.

(14) Kresse, G.; Joubert, J. *Phys. Rev. B* **1999**, *59*, 1758.

(15) (a) Kresse, G.; Hafner, J. *Phys. Rev. B* **1993**, *47*, 558. (b) Kresse, G.; Furthmuller, J. *Comput. Mater. Sci.* **1996**, *6*, 15–50. (c) Phys. Rev. B 1996, 54, 11169.

(16) Graciani, J.; Álvarez, L. J.; Rodriguez, J. A.; Sanz, J. F. *J. Phys. Chem. C* **2008**, *112*, 2624.

(17) Liu, P.; Rodriguez, J. A. *J. Chem. Phys.* **2007**, *126*, 164705.

(18) Delley, B. *J. Chem. Phys.* **1990**, *92*, 508. 2002113, 7756.

(19) Halgren, T. A.; Lipscomb, W. N. *Chem. Phys. Lett.* **1977**, *49*, 225.

(20) (a) Rodriguez, J. A.; Liu, P.; Viñes, F.; Illas, F.; Takahashi, Y.; Nakamura, K. *Ang. Chem. Int. Ed.* **2008**, *47*, 6685. (b) Rodriguez, J. A.; Liu, P.; Viñes, F.; Illas, F.; Takahashi, Y.; Nakamura, K. *J. Chem. Phys.* **2007**, *127*, 211102.

(21) (a) Rodríguez, J. A.; Liu, P.; Gomes, J.; Nakamura, K.; Viñes, F.; Sousa, C.; Illas, F. *Phys. Rev. B* **2005**, *72*, 075427. (b) Viñes, F.; Sousa, C.; Liu, P.; Rodriguez, J. A.; Illas, F. *J. Chem. Phys.* **2005**, *122*, 174709. (c) Viñes, F.; Sousa, C.; Illas, F.; Liu, P.; Rodriguez, J. A. *J. Phys. Chem. C* **2007**, *111*, 1307.

(22) Walden, M.; Lai, X.; Goodman, D. W. *Science* **1998**, *281*, 1647.

(23) Maeda, Y.; Fujitani, T.; Tsubota, S.; Haruta, M. *Surf. Sci.* **2004**, *562*, 1.

(24) Remediakis, I. N.; Lopez, N.; Nørskov, J. K. *Angew. Chem., Int. Ed.* **2005**, *44*, 1824.

(25) Matthey, D.; Wang, J. G.; Wendt, S.; Matthiesen, J.; Schaub, R.; Lægsgaard, E.; Hammer, B.; Besenbacher, F. *Science* **2007**, *315*, 1692.

(26) Zhou, J.; Kang, Y. C.; Chen, D. A. *Surf. Sci.* **2003**, *537*, L429−L434.

(27) Remediakis, I. N.; Lopez, N.; Nørskov, J. K. *Appl. Catal., A* **2005**, *291*, 13.

(28) Bader, R. F. W. *Atoms in Molecules: A Quantum Theory*; Oxford University Press: Oxford, U.K., 1990.

(29) Nakamura, J.; Campbell, J. M.; Campbell, C. T. *J. Chem. Soc., Faraday Trans.* **1990**, *86*, 2725.

(30) Wang, X.; Rodriguez, J. A.; Hanson, J. C.; Gamarra, D.; Martinez-Arias, A.; Fernandez-Garcia, M. *Top. Catal.* **2008**, *49*, 81.

(31) Clausen, B. S.; Steffensen, G.; Fabius, B.; Villadsen, J.; Feidenhansl, R.; Topsøe, H. *J. Catal.* **1991**, *132*, 524.

(32) Rodriguez, J. A.; Hanson, J. C.; Wen, W.; Wang, X.; Brito, J. L. *Catal. Today*, **2009**; in press.

(33) Panagiotopoulou, P.; Kondarides, D. I. *Catal. Today* **2006**, *112*, 49.

(34) Panagiotopoulou, P.; Christodoulakis, A.; Kondarides, D. I.; Boghosian, S. *J. Catal.* **2006**, *240*, c114.

(35) Gokhale, A. A.; Dumesic, J. A.; Mavrikakis, M. *J. Am. Chem. Soc.* **2008**, *130*, 1402.

(36) Henderson, M. A. *Surf. Sci. Reports* **2002**, *46*, 5–308.

(37) Oviedo, J.; Sánchez-de-Armas, R.; San Miguel, M. A.; Sanz, J. F. *J. Phys. Chem. C.* **2008**, *112*, 17739.

(38) Wu, T.; Kaden, W. E.; Anderson, S. L. *J. Phys. Chem. C* **2008**, *112*, 9006.

JP900483U